Supporting Information

Modification-Free Fabricating Ratiometric Nanoprobe Based on Dual Emissive Carbon Dots for Nitrite Determination in Food Samples

Juanjuan Liu,[†‡] Yonglei Chen*[†‡] Lili Wang,[†‡] Min Na,[†‡] Hongli Chen,[†‡] and Xingguo Chen*[†‡§]

[†] State Key Laboratory of Applied Organic Chemistry, Lanzhou University, Lanzhou 730000, China

[‡] Department of Chemistry, Lanzhou University, Lanzhou 730000, China

[§] Key Laboratory of Nonferrous Metal Chemistry and Resources Utilization of Gansu Province, Lanzhou University, Lanzhou 730000, China

* Corresponding author

E-mail address: chenxg@lzu.edu.cn (X-G Chen)

chenyl@lzu.edu.cn (Y-L Chen)

Tel: 86-931-8912763; Fax: 86-931-8912582

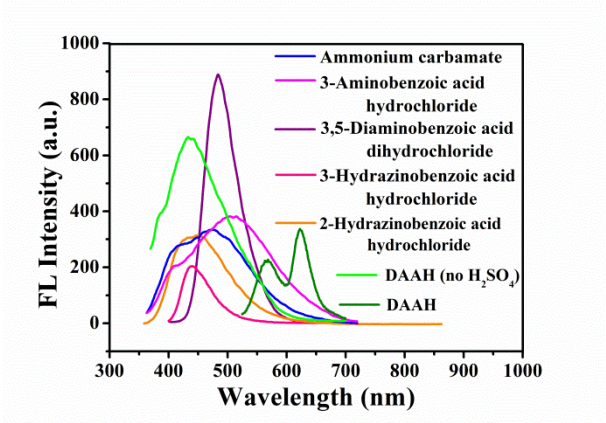

17

18 **Figure S1.** Fluorescence spectra of the CDs prepared through using different carbon

19 sources and H_2SO_4 for CDs.

20

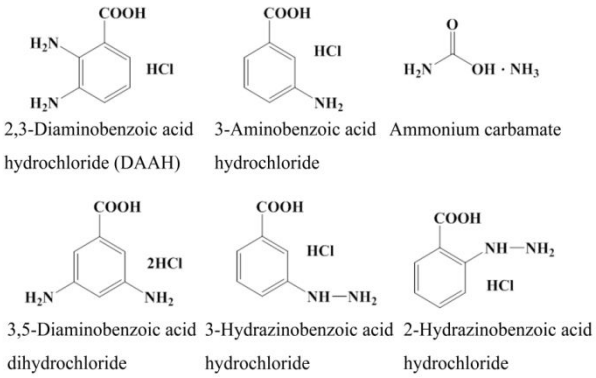

21

22 **Figure S2.** Structural formulas of DAAH, 3-aminobenzoicacid hydrochloride,

23 ammounium carbamate, 3,5-diaminobenzoic acid dihydrochloride,

24 3-hydrazinobenzoic acid hydrochloride, and 2-hydrazinobenzoic acid hydrochloride,

25 respectively.

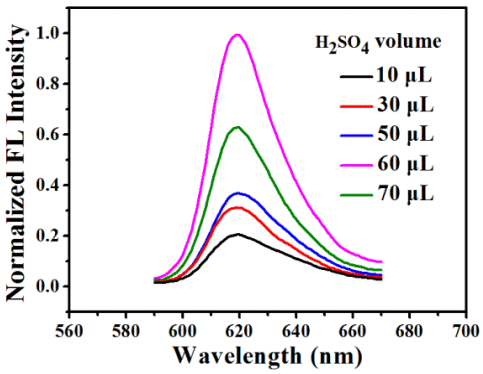

27

28 **Figure S3.** Effect of different volume of H_2SO_4 (98%) on the fluorescence intensity

29 of the RYDE CDs.

30

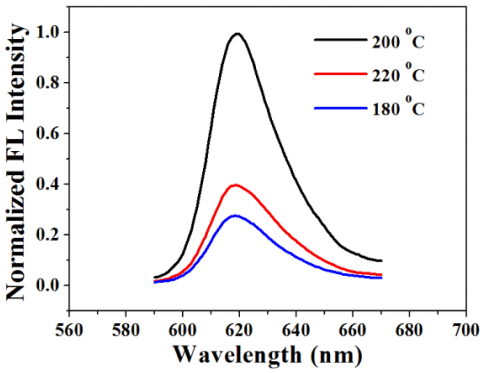

31

32 **Figure S4.** Effect of different carbonization temperature on the fluorescence intensity

33 of the RYDE CDs.

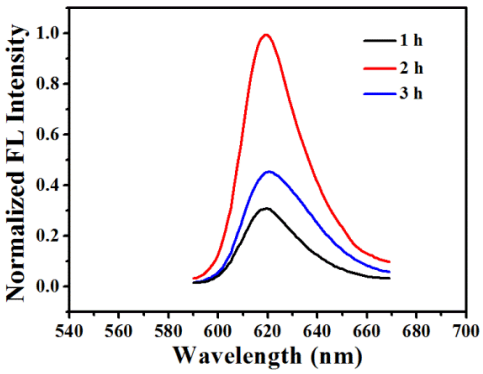

35

36 **Figure S5.** Effect of different carbonization time on the fluorescence intensity of the

37 RYDE CDs.

38

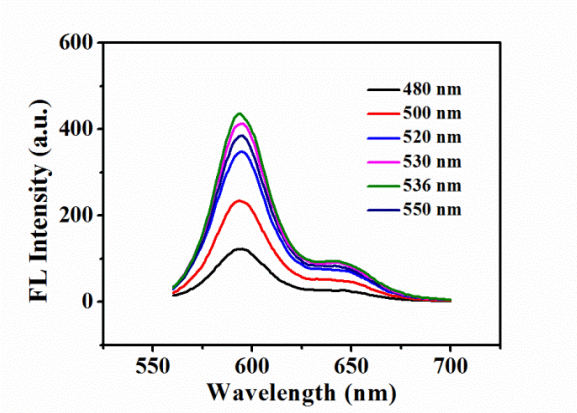

39

40 **Figure S6.** Fluorescence spectra scanned under different excitation wavelength of the

41 RODE CDs.

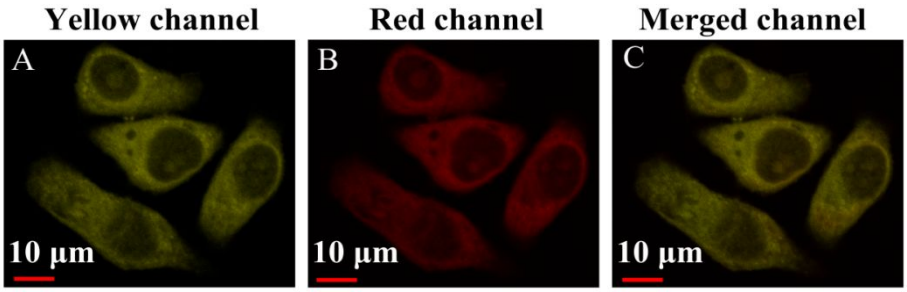

Figure S7. Confocal microscopy fluorescence images of HeLa cells treated with the RYDE CDs (208 μg/mL) in yellow channel, red channel and the merged image of the two channels.

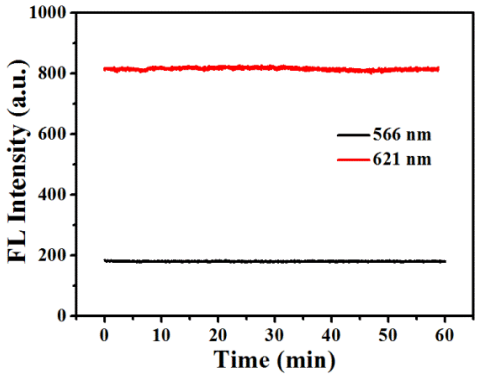

Figure S8. Fluorescence intensity variation of the RYDE CDs as a function of illumination time.

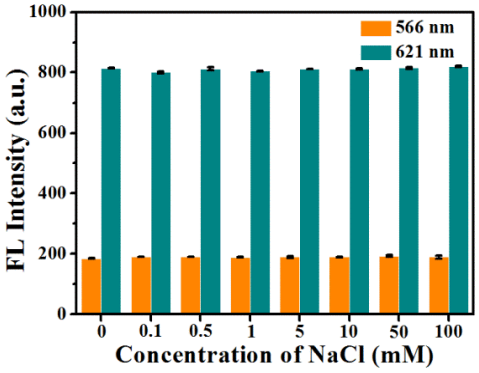

Figure S9. Fluorescence intensity variation of the RYDE CDs as a function of NaCl concentrations. Three replicate measurements were completed for each point.

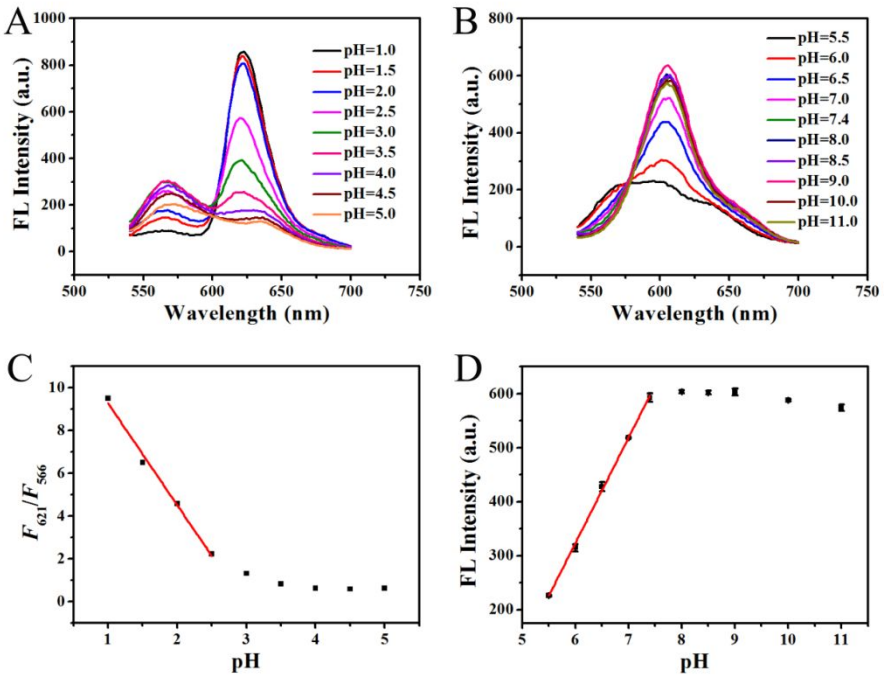

Figure S10. Fluorescence spectra of the RYDE CDs probe under (A) acid and (B) alkaline pH conditions. Effect of pH of buffer solution on the (C) fluorescence intensity ratio (F_{621}/F_{566}) and the (D) fluorescence intensity centered at 605 nm of the RYDE CDs solution.

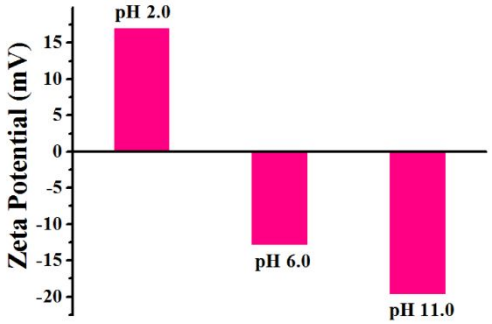

Figure S11. The zeta potential histogram of RYDE CDs under different pH conditions.

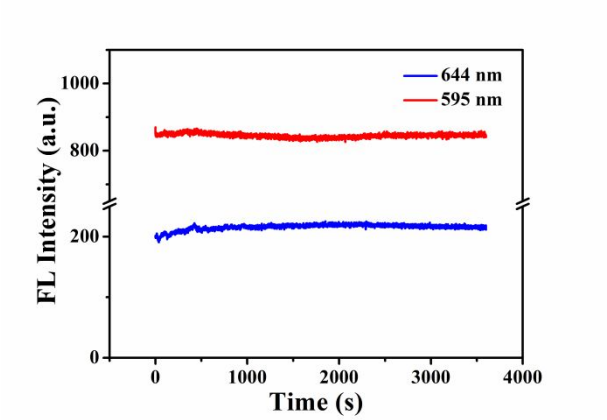

Figure S12. Fluorescence intensity variation of the RODE CDs as a function of illumination time.

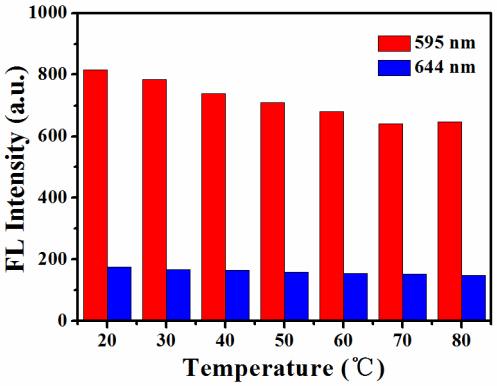

Figure S13. Fluorescence intensity variation of the RODE CDs as a function of temperature.

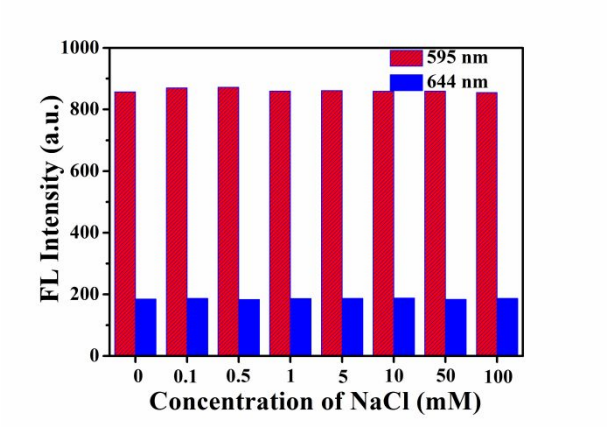

Figure S14. Fluorescence intensity variation of the RODE CDs as a function of NaCl concentrations.

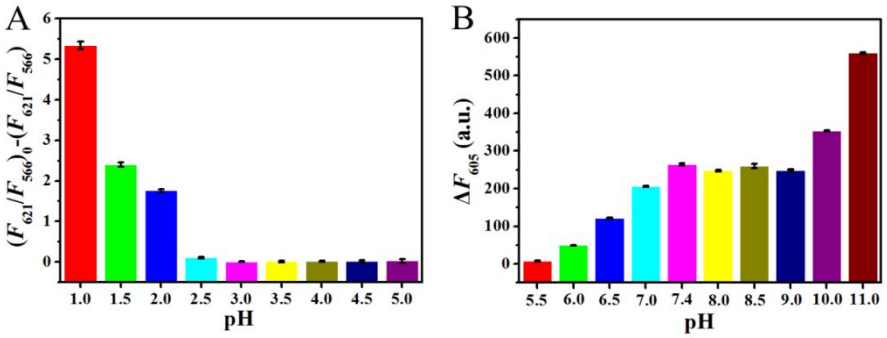

Figure S15. Effect of pH of buffer solution on $(F_{621}/F_{566})_0$-(F_{621}/F_{566}) and ΔF_{605}. $(F_{621}/F_{566})_0$ and (F_{621}/F_{566}) were the fluorescence intensity of the RYDE CDs solution in the absence and presence of 50 μM nitrite, ΔF_{605} was the difference of the fluorescence intensity centered at 605 nm in the absence and presence of 50 μM nitrite, respectively. Three replicate measurements were completed for each point.

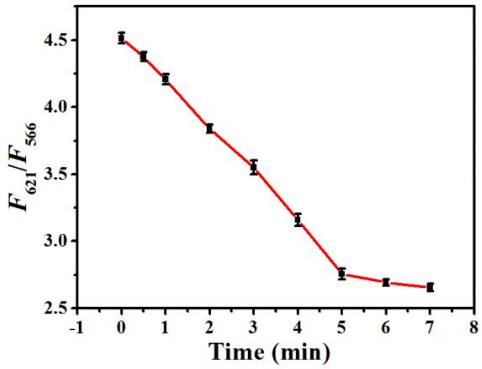

Figure S16. Effect of response time on F_{621}/F_{566}. F_{621} and F_{566} were the fluorescence intensity of the RYDE CDs solution at 621 nm and 566 nm in the presence of 50 μM nitrite, respectively. Three replicate measurements were completed for each point.

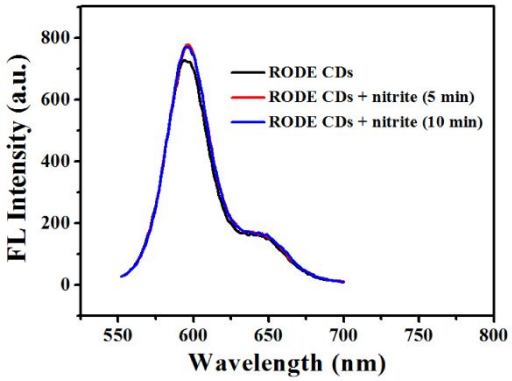

Figure S17. Fluorescence spectra of RODE CDs in ethanol solution in the absence and presence (5 min or even 10 min) of 3.0 mM nitrite.

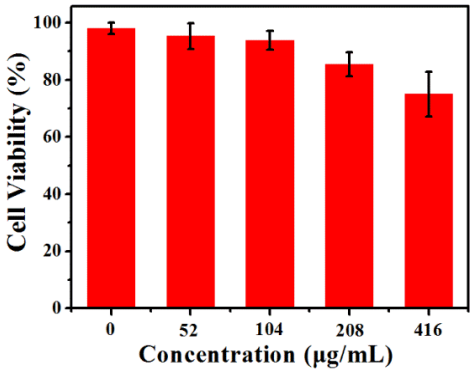

Figure S18. Cell viability of the HeLa cells under different concentrations (0, 52, 104, 208, 416 μg/mL) of the RYDE CDs. Three replicate measurements were completed for each point.

Table S1. Comparison of the properties of the RYDE CDs with other CDs.

Synthetic raw material	Preparation temperature (℃)	Preparation time (h)	Kind of CDs	Excitation wavelength (nm)	Emission wavelength (nm)	QY	Ref.
ascorbic acid, ethylene glycol	160/180	2	one	365	435/538	not mentioned	1
m-phenylenediamine, sulfuric acid	200	10	one	300	360/520	43%* (460 nm excitation)	2
m-aminophenol, oxalic acid	180	12	one	380	430/510	5.40% (380 nm excitation)	3
o-phenylenediamine, phosphoric acid	200	24	one	380	440/640	14.88%	4
2,5-diaminotoluene sulfate	150	12	one	380	525/603	9.00% (380 nm excitation)	5
DAAH	200	2	two	520 535	566/621 595/644	8% 18%	this work

*: The QY was measured under 460 nm excitation wavelength, rather than 300 nm. When excited at 460 nm, the CDs might be single emissive.

Table S2. Comparison of different kinds of CDs probes for the detection of nitrite.

Type of probe	Detection wavelength (nm)	Linear range (μM)	Limit of detection (nM)	Ref.
CDs-neutral red	520	0-4.34	0.518	6
N,P-CDs	530	0.01-0.09	3.3	7
N-CDs	390	15-1110	13500	8
N,P-GQDs	470	0.005-0.03	2.5	9
N-CDs	417	0-1000	1000	10
RYDE CDs	566/621	0.1-100	31.61	this work

102 **Table S3.** The quenching parameters in Stern-Volmer equation.

T (K)	Equation	R^2	K_{sv} ($L \cdot mol^{-1}$)	K_q ($L \cdot mol^{-1} \cdot s^{-1}$)
288	$(F_{621}/F_{566})_0/(F_{621}/F_{566})$ $=0.9963+1.274\times10^{-2}[\ NO_2^-\ ]$	0.992	1.274×10^4	8.85×10^{12}
303	$(F_{621}/F_{566})_0/(F_{621}/F_{566})$ $=0.9922+1.124\times10^{-2}[\ NO_2^-\ ]$	0.993	1.124×10^4	7.81×10^{12}
313	$(F_{621}/F_{566})_0/(F_{621}/F_{566})$ $=0.9863+1.014\times10^{-2}[\ NO_2^-\ ]$	0.993	1.014×10^4	7.04×10^{12}

103

Quantum yield (QY) measurements.

QY of the obtained RYDE CDs and RODE CDs was determined by the method mentioned in our previous work.[11] The absolute fluorescence quantum yield can be simply represented in the equation below:

$$\mathrm{QY} = \frac{\int L_{\mathrm{emission}}}{\int E_{\mathrm{solvent}} - \int E_{\mathrm{sample}}} \qquad (1)$$

where QY was the absolute quantum yield, L_{emission} was the fluorescence (FL) emission spectrum of the sample, collected using the sphere; E_{sample} was the spectrum of the light used to excite the sample, collected using the sphere; E_{solvent} was the spectrum of the light used for excitation with only the solvent in the sphere, collected using the sphere. The solvent for RYDE CDs and RODE CDs were deionized water and ethanol, respectively.

REFERENCES

1. Mohan, R.; Drbohlavova, J.; Hubalek, J. Dual band emission in carbon dots. *Chem. Phys. Lett.* **2018,** *692*, 196-201.

2. Zhou, W.; Zhuang, J.; Li, W.; Hu, C.; Lei, B.; Liu, Y. Towards efficient dual-emissive carbon dots through sulfur and nitrogen co-doped. *J. Mater. Chem. C* **2017,** *5*, 8014-8021.

3. Ma, Y.; Chen, Y.; Liu, J.; Han, Y.; Ma, S.; Chen, X. Ratiometric fluorescent detection of chromium(VI) in real samples based on dual emissive carbon dots. *Talanta* **2018,** *185*, 249-257.

4. Song, W.; Duan, W.; Liu, Y.; Ye, Z.; Chen, Y.; Chen, H.; Qi, S.; Wu, J.; Liu, D.; Xiao, L.; Ren, C.; Chen, X. Ratiometric detection of intracellular lysine and pH with one-pot synthesized dual emissive carbon dots. *Anal. Chem.* **2017,** *89*, 13626-13633.

5. Liu, J.; Dong, Y.; Ma, Y.; Han, Y.; Ma, S.; Chen, H.; Chen, X. One-step synthesis of red/green dual-emissive carbon dots for ratiometric sensitive $ONOO^-$ probing and cell imaging. *Nanoscale* **2018,** *10*, 13589-13598.

6. Hu, X.; Shi, J.; Shi, Y.; Zou, X.; Tahir, H. E.; Holmes, M.; Zhang, W.; Huang, X.; Li, Z.; Xu, Y. A dual-mode sensor for colorimetric and fluorescent detection of nitrite in hams based on carbon dots-neutral red system. *Meat Sci.* **2019,** *147*, 127-134.

7. Zan, M.; Rao, L.; Huang, H.; Xie, W.; Zhu, D.; Li, L.; Qie, X.; Guo, S. S.; Zhao, X. Z.; Liu, W.; Dong, W. F. A strong green fluorescent nanoprobe for highly sensitive and selective detection of nitrite ions based on phosphorus and nitrogen co-doped carbon quantum dots. *Sensor. Actuat. B: Chem.* **2018,** *262*, 555-561.

8. Karali, K. K.; Sygellou, L.; Stalikas, C. D. Highly fluorescent N-doped carbon nanodots as an effective multi-probe quenching system for the determination of nitrite, nitrate and ferric ions in food matrices. *Talanta* **2018,** *189*, 480-488.

9. Liu, R.; Zhao, J.; Huang, Z.; Zhang, L.; Zou, M.; Shi, B.; Zhao, S. Nitrogen and phosphorus co-doped graphene quantum dots as a nano-sensor for highly sensitive and selective imaging detection of nitrite in live cell. *Sensor. Actuat. B: Chem.* **2017,** *240*, 604-612.

10. Zhang, H.; Kang, S.; Wang, G.; Zhang, Y.; Zhao, H. Fluorescence determination of nitrite in water using prawn-shell derived nitrogen-doped carbon nanodots as fluorophores. *ACS Sens.* **2016,** *1*, 875-881.

11. Feng, J.; Chen, Y.; Han, Y.; Liu, J.; Ren, C.; Chen, X. Fluorescent carbon nanoparticles: A low-temperature trypsin-assisted preparation and Fe^{3+} sensing. *Anal. Chim. Acta* **2016,** *926*, 107-117.